Inorg. Chem. **2002**, *41*, 3017–3024

Synthesis and Characterization of Redox-Active Coordination Polymers Generated from Ferrocene-Containing Bridging Ligands

Ryo Horikoshi,[†] Tomoyuki Mochida,*[,†,‡] and Hiroshi Moriyama[†]

Department of Chemistry, Faculty of Science, Toho University, Funabashi, Chiba, Japan 274-8510, and PRESTO, Japan Science and Technology Corporation, Japan

Received November 16, 2001

Coordination polymers showing redox activity have been constructed by using ferrocene-based bidentate ligands, 1,1′-(4-dipyridinethio)ferrocene (**1**) and 1,1′-(2-dipyridinethio)ferrocene (**2**). The ligand of **1** formed an Ag^{I} coordination polymer, **1**·$AgPF_6$·$(CH_3CN)_2$ (**3**). This complex showed a 1-D double-chain structure, with a weak interchain Ag···Ag interaction. Combination of **1** with $M(hfac)_2$ (M = Mn, Cu, Zn) afforded 1-D chain complexes, **1**·$M(hfac)_2$ (M = Mn (**5**), Cu (**6**), Zn (**7**)). The complex **2**·$CuPF_6$ (**8**) showed a 1-D twisted helix-like chain structure.

Introduction

The design and syntheses of supramolecular coordination polymers, constructed from multifunctional ligands and transition metals, have been extensively explored over the past decade.[1] One of the strategies for developing topologically interesting coordination polymers is to exploit pyridine-derived bidentate ligands bearing rigid or flexible spacers such as CH−CH, C═C, N−N, S−S, and alkyl groups.[2] From the viewpoint of constructing functional supramolecular compounds, it may be interesting to incorporate functional groups on the ligand instead of such spacers.[3] For example, redox-active coordination polymers are intriguing targets for us, because redox functions may lead to a variety of interesting electrical, photophysical, or catalytic phenomena.[4] Our approach to producing redox-active coordination polymers is to incorporate redox-active moieties on the bridging ligand. Along this line, we have designed here the ferrocene-based bidentate ligands, 1,1′-(4-dipyridinethio)ferrocene (**1**) and 1,1′-(2-dipyridinethio)ferrocene (**2**) (Chart), although the synthesis of ligand **2** was reported independently by Laguna et al. very recently.[5] Ferrocenes not only show good redox activity but also play important roles in the field of materials science, as components of catalysts, molecular magnets, and nonlinear optical materials.[6] In addition, introducing fer-

* To whom correspondence should be addressed. E-mail: mochida@chem.sci.toho-u.ac.jp.

[†] Toho University.

[‡] PRESTO.

(1) (a) Leininger, S.; Olenyuk, B.; Stang, P. J. *Chem. Rev.* **2000**, *100*, 853−908. (b) Swiegers, G. F.; Malefetse, T. J. *Chem. Rev.* **2000**, *100*, 3483−3537. (c) Fujita, M. *Chem. Soc. Rev.* **1998**, *27*, 417−425. (d) Zaworotko, M. J. *Chem. Commun.* **2001**, 1−9. (e) Kitagawa, S.; Kondo, M. *Bull. Chem. Soc. Jpn.* **1998**, *71*, 1739−1753. (f) Day, P. *Chem. Commun.* **2000**, 3483−3488. (g) Moulton, B.; Zaworotko, M. J. *Chem. Rev.* **2001**, *101*, 1629−1658. (h) Batten, S. R. *CrystEngComm* **2001**, *18*, 1−7. (i) Hagrman, P. J.; Hagrman, D.; Zubieta, J. *Angew. Chem., Int. Ed.* **1999**, *38*, 2638−2684.

(2) (a) Fujita, M.; Sasaki, O.; Mitsuhashi, T.; Fujita, T.; Yazaki, J.; Yamaguchi, K.; Ogura, K. *Chem. Commun.* **1996**, 1535−1536. (b) Fujita, M.; Aoyagi, M.; Ogura, K. *Inog. Chim, Acta* **1996**, *246*, 53−57. (c) Plater, M. J.; Foreman, M. R. St. J.; Gelbrich, T.; Coles, S. J. *J. Chem. Soc., Dalton Trans.* **2000**, 3065−3073. (d) Dong, Y.-B.; Layland, R. C.; Smith, M. D.; Pschirer, N. G.; Bunz, U. H. H.; zur Loye, H.-C. *Inorg. Chem.* **1999**, *38*, 3056−3060. (e) Tong, M.-L.; Ye, B.-H.; Cai, J.-W.; Chen, X.-M.; Ng, S. W. *Inorg. Chem.* **1998**, *37*, 2645−2650. (f) Carlucci, L.; Ciani, G.; Proserpio, D. M. *J. Chem. Soc., Dalton Trans.* **1999**, 1799−1804. (g) Fujita, M.; Aoyagi, M.; Ogura, K. *Bull. Chem. Soc. Jpn.* **1998**, *71*, 1799−1804. (h) Lu, J. Y.; Babb, A. *Inorg. Chim. Acta* **2001**, *318*, 186−190. (i) Plater, M. J.; Foreman, M. R. St. J.; Howie, R. A.; Skakle, J. M. S. *Inorg. Chim. Acta* **2000**, *318*, 175−180. (j) Plater, M. J.; Foreman, M. R. St. J.; Gelbrich, T.; Hursthouse, M. B. *Inorg. Chim. Acta* **2001**, *318*, 171−174. (k) Hagrman, D.; Sangregorio, C.; O'Conor, C. J.; Zubieta, J. *J. Chem. Soc., Dalton Trans.* **1998**, 3707−3709. (l) De Munno, G.; Armentano, D.; Poerio, T.; Julve, M.; Real, J. A. *J. Chem. Soc., Dalton Trans.* **1998**, 1813−1817. (m) Real, J. A.; Andrés, E.; Muñoz, M. C.; Julve, M.; Granier, T.; Bousseksou, A.; Varret, F. *Science* **1995**, *268*, 265−267. (n) Noro, S.; Kondo, M.; Ishii, T.; Kitagawa, S.; Matsuzaka, H. *J. Chem. Soc., Dalton Trans.* **1999**, 1569−1574. (o) Kondo, M.; Shimamura, M.; Noro, S.; Kimura, Y.; Uemura, K.; Kitagawa, S. *J. Solid State Chem.* **2000**, *152*, 113−119. (p) Lu, J. Y.; Babb, A. M. *Inorg. Chem.* **2001**, *40*, 3261−3262.

(3) (a) Fujita, N.; Biradha, K.; Fujita, M.; Sakamoto, S.; Yamaguchi, K. *Angew. Chem., Int. Ed.* **2001**, *40*, 1718−1721. (b) Abrahams, B. F.; Hoskins, B. F.; Michail, D. M.; Robson, R. *Nature* **1994**, *369*, 727−729. (c) Lin, K.-J. *Angew. Chem., Int. Ed.* **1999**, *38*, 2730−2732. (d) Sharma, C. V. K.; Broker, G. A.; Huddleston, J. G.; Baldwin, J. W.; Metzger, R. M.; Rogers, R. D. *J. Am. Chem. Soc.* **1999**, *121*, 1137−1144.

(4) (a) Audrieux, C. P.; Bolcman, C.; D.-Bouchiat, J. M.; M'Halla, F.; Saveant, J. M. *J. Am. Chem. Soc.* **1980**, *102*, 3806−3813. (b) Audrieux, C. P.; Haas, O.; Saveant, J. M. *J. Am. Chem. Soc.* **1986**, *108*, 8175−8182. (c) Balzani, V.; Juris, A.; Venturi, M.; Campagna, S.; Serroni, S. *Chem. Rev.* **1996**, *96*, 759−833.

(5) Barranco, E. M.; Crespo, O.; Gimeno, M. C.; Jones, P. G.; Laguna, A.; Sarroca, C. *J. Chem. Soc., Dalton Trans.* **2001**, 2523−2529.

10.1021/ic011176k CCC: $22.00
Published on Web 05/01/2002

Chart 1. Bridging Ligands of 1,1′-(4-Dipyridinethio)ferrocene (**1**), 1,1′-(2-Ddipyridinethio)ferrocene (**2**), and Their Coordination Polymer Complexes (**3**−**8**)

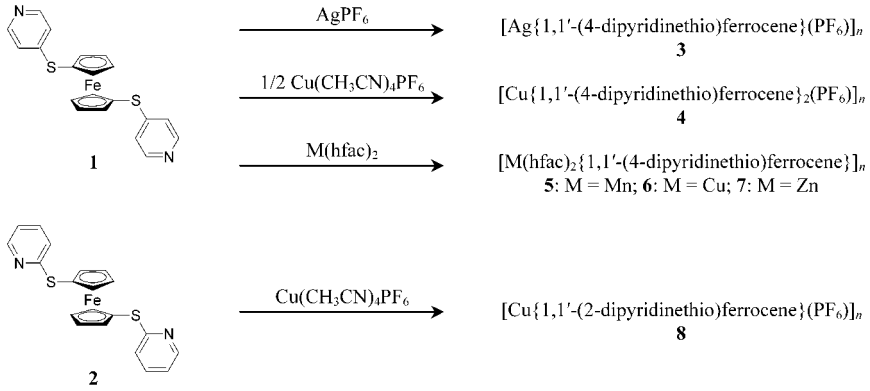

rocene derivatives to coordination polymers may lead to interesting assembled structures because of the conformational flexibility of the ferrocenyl rings. So far, several groups have reported the synthesis of versatile ligands of dppf analogues and their interesting coordination polymers,[7] although these ligands tend to afford chelate or *molecular* compounds.

On the other hand, the control of assembled structures can be achieved by selecting appropriate metal ions with specific coordination geometries. To obtain coordination polymers, bidentate ligands **1** and **2** were combined with metal ions bearing two coordination sites, Ag^I, Cu^I, and $M(hfac)_2$. The coordination chemistries of Ag^I and Cu^I ions are well documented; these ions show a variety of coordination environments, for example, linear, T-shaped, and tetrahedral.[8] The $M(hfac)_2$ (M = first row transition metal, hfac = hexafluoroacetylacetonate) species are also useful building blocks for coordination polymers.[9] In the present paper, we report the syntheses, structures, and electrochemical properties of the ferrocene containing bridging ligands and their coordination polymer complexes, **1**·$AgPF_6$·$(CH_3CN)_2$ (**3**), $\mathbf{1}_2$·$CuPF_6$ (**4**), **1**·$M(hfac)_2$ (M = Mn(**5**), Cu(**6**), Zn(**7**)), and **2**·$CuPF_6$ (**8**).

Experimental Section

Materials and Instrumentation. All reagents and solvents were commercially available except for $[Cu(CH_3CN)_4]PF_6$[10] and 1,1′-dilithioferrocene,[11] which were synthesized by following the literature procedures. NMR spectra were recorded on a Bruker AC-250 spectrometer. Infrared spectra were recorded on a JASCO FT-IR 230 spectrometer as KBr pellets in the 4000−400 cm^{-1} range.

(6) (a) Plenio, H.; Aberle, C.; Shihadeh, Y. A.; Lloris, J. M.; Máñez, R. M.; Pardo, T.; Soto, J. *Chem.*—*Eur. J*. **2001**, *7*, 2848−2861. (b) Jutzi, P.; Lenze, N.; Neumann, B.; Stammler, H.-G. *Angew. Chem., Int. Ed*. **2001**, *40*, 1424−1427. (c) Miller, J. S.; Epstein, A. J.; Reiff, W. M. *Acc. Chem. Res*. **1988**, *21*, 114−120. (d) Farrell, T.; Friedrichsen, T. M.; Malessa, M.; Haase, D.; Saak, W.; Asselberghs, I.; Wostyn, K.; Clays, K.; Persoons, A.; Heck, J.; Manning, A. R. *J. Chem. Soc., Dalton Trans*. **2001**, 29−36. (e) *Ferrocenes: Homogeneous Catalysis, Organic Synthesis, Materials science*; Togni, A., Hayashi, T., Eds.; VCH: Weinheim, 1995. (f) Long, N. J. *Metallocenes: An Introduction to Sandwich Complexes*; Blackwell Science Inc.: Cambridge, MA, 1998. (g) Bradley, S.; Camm, K. D.; Liu, X.; McGowan, P. C.; Mumtaz, R.; Oughton, K. A.; Podesta, T. J.; Thomton-Pett, M. *Inorg. Chem.* **2002**, *41*, 715−726.

(7) (a) Chen-jie, F.; Chun-ying, D.; Cheng, H.; Qing-jin, M. *Chem. Commun*. **2000**, 1187−1188. (b) Christie, S. D.; Subramanian, S.; Thompson, L. K.; Zaworotko, M. J. *J. Chem. Soc., Chem. Commun*. **1995**, 2563−2564. (c) Crespo, O.; Gimeno, M. C.; Jones, P. G.; Laguna, A.; Sarroca, C. *Chem. Commun*. **1998**, 1481−1482. (d) Crespo, O.; Canales, F.; Gimeno, M. C.; Jones, P. G.; Laguna, A. *Organometallics* **1999**, *18*, 3142−3148. (e) Canales, S.; Crespo, O.; Gimeno, M. C.; Jones, P. G.; Laguna, A. *J. Organomet. Chem*. **2000**, *613*, 50−55. (f) Gimeno, M. C.; Jones, P. G.; Laguna, A.; Sarroca, C.; Villacampa, M. D. *Inorg. Chim. Acta*, **2001**, *316*, 89−93. (g) Grosche, M.; Herdtweck, E.; Peters, F.; Wagner, M. *Organometallics* **1999**, *18*, 4669−4672. (h) Pienio, H.; Burth, D.; Gockel, P. *Chem. Ber*. **1993**, *126*, 2585−2590. (i) Houlton, A.; Mingos, D. M. P.; Murphy, D. M.; Williams, D. J.; Phang, L.-T.; Hor, T. S. A.; *J. Chem. Soc., Dalton Trans*. **1993**, 3629−3630. (j) Fontani, M.; Peters, F.; Scherer, W.; Wachter, W.; Wagner, M.; Zanello, P. *Eur. J. Inorg. Chem*. **1998**, 1453−1456.

(8) (a) Munakata, M.; Wu, L.-P.; Kuroda-Sowa, T. *Adv. Inorg. Chem.* **1999**, *46*, 173−303. (b) Rarig, R. S.; Zubieta, J. *Inorg. Chim. Acta* **2001**, *319*, 235−239. (c) Munakata, M.; Wen, M.; Suenaga, Y.; Kuroda-Sowa, T.; Maekawa, M.; Anahata, M. *Polyhedron* **2001**, *20*, 2321−2327. (d) Hanton, L. R.; Lee, K. *J. Chem. Soc., Dalton Trans*. **2000**, 1161−1166. (e) Munakata, M.; Wen, M.; Suenaga, Y.; Kuroda-Sowa, T.; Maekawa, M.; Anahata, M. *Polyhedron* **2001**, *20*, 2037−2043. (f) Venkataraman, D.; Lee, S.; Moore, J. S.; Zhang, P.; Hirsch, K. A.; Gardner, G. B.; Covey, A. C.; Prentice, C. L. *Chem. Mater*. **1996**, *8*, 2030−2040. (g) LaDuca, R. L., Jr.; Rarig, R. S., Jr.; Zapf, P. J.; Zubieta, J. *Solid State Sci.* **2000**, *2*, 39−45. (h) Ino, I.; Zhong, J. C.; Munekata, M.; Kuroda-Sowa, T.; Maekawa, M.; Suenaga, Y.; Kitamori, Y. *Inorg. Chem*. **2000**, *39*, 4273−4279. (i) Suenaga, Y.; Kuroda-Sowa, T.; Munekata, M.; Maekawa, M. *Polyhedron* **1998**, *18*, 191−195. (j) Calucci, L.; Ciani, G.; Proserpio, D. M. *Chem. Commun*. **1999**, 449−450. (k) Tong, M.-L.; Zheng, S.-L.; Chen, X.-M. *Chem. Commun*. **1999**, 561−562. (l) Maekawa, M.; Konaka, H.; Suenaga, Y.; Kuroda-Sowa, T.; Munakata, M. *J. Chem. Soc., Dalton Trans*. **2000**, 4160−4166. (m) Calucci, L.; Ciani, G.; Proserpio, D. M.; Sironi, A. *Inorg. Chem*. **1998**, *37*, 5941−5943. (n) Carlucci, L.; Ciani, G.; Proserpio, D. M.; Sironi, A. *J. Am. Chem. Soc*. **1995**, *117*, 4562−4569. (o) Suenaga, Y.; Kamiya, T.; Kuroda-Sowa, T.; Maekawa, M.; Munakata, M. *Inorg. Chim. Acta* **2000**, *308*, 17−21. (p) Carlucci, L.; Ciani, G.; Proserpio, D. M.; Sironi, A. *Angew. Chem., Int. Ed. Engl*. **1995**, *34*, 1895−1897. (q) Hong, M.; Su, W.; Cao, R.; Fujita, M.; Lu, J. *Chem.*—*Eur. J*. **2000**, *6*, 427−431. (r) Blake, A. J.; Champness, N. R.; Chung, S. S. M.; Li, W.-S.; Schröder, M. *Chem. Commun*. **1997**, 1675−1676. (s) Zhang, J.; Xiong, R.-G.; Zuo, J.-L.; Che, C.-M.; You, X.-Z. *J. Chem. Soc., Dalton Trans*. **2000**, 2898−2900. (t) Chen, Z.-F.; Xiong, R.-G.; Zhang, J.; Zuo, J.-L.; You, X.-Z.; Che, C.-M.; Fun, H.-K. *J. Chem. Soc., Dalton Trans*. **2000**, 4010−4012. (u) Plasseraud, L.; Maid, H.; Hampel, F.; Saalfrank, F. *Chem* −*Eur. J*. **2001**, *7*, 4007−4011. (v) Horikoshi, R.; Mochida, T.; Maki, N.; Yamada, S.; Moriyama, H. *J. Chem. Soc., Dalton Trans*. **2002**, 28−33.

(9) (a) Horikoshi, R.; Mochida, T.; Moriyama, H. *Inorg. Chem*. **2001**, *40*, 2430−2433. (b) Mago, G.; Hinago, M.; Miyasaka, H.; Matsumoto, N.; Okawa, H. *Inorg. Chim. Acta* **1997**, *254*, 145−150. (c) Dong, Y.-B.; Smith, M. D.; Layland, R. C.; zur Loye, H.-C. *Inorg. Chem*. **1999**, *38*, 5027−5033. (d) Shen, H.-Y.; Liao, D.-Z.; Jiang, Z.-H.; Yan, S.-P.; Sun, B.-W.; Wang, G.-L.; Yao, X.-K.; Wang, H.-G. *Polyhedron* **1998**, *17*, 1953−1957.

(10) Kubas, G. J. *Inorg. Synth*. **1979**, *19*, 90−92.

(11) Balavoine, G. G. A.; Doisneau, G.; F.-Khan, T. *J. Organomet. Chem*. **1991**, *412*, 381−382.

Cyclic voltammograms were recorded with an ALS/chi electrochemical analyzer model 600A. Solution state measurements were performed in dichloromethane solutions containing 0.1 mol dm^{-3} nBu_4NClO_4 as the supporting electrolyte, at a scan rate of 0.2 V s^{-1}, with Ag/Ag^+ electrode as a reference. A working electrode of a glassy carbon disk was used. Solid-state voltammograms[2n,o] were measured by using a carbon-paste working electrode; well-ground mixtures of each bulk sample and carbon paste (graphite and mineral oil) were set in a cavity on a Teflon rod and connected to a platinum wire. A platinum-wire counter electrode and a Ag/AgCl reference electrode were used. Measurements were performed by using a three-electrode system in 0.1 mol dm^{-3} $NaClO_4$ aqueous solutions at a scan rate of 0.2 V s^{-1}, in the range 0−1.5 V. Thermogravimetric analysis was performed on MAC SCIENCE TG DTA 2000. Solid-state UV−vis spectra were recorded on a JASCO V570 UV−vis−NIR spectrophotometer. Emission spectra were obtained on a HITACHI F4500 fluorescence spectrophotometer. The magnetic susceptibilities were measured by means of a Quantum Design MPMS-2 SQUID susceptometer in the temperature range 2−300 K at a constant field of 1000 mT. Elemental analyses were performed on a Yanagimoto C−H−N corder (MT-3).

1,1′-(4-Dipyridinethio)ferrocene (1). A solution of 4,4′-dipyridyl disulfide (1.6 g, 7.4 mmol) in THF (40 mL) was added at −80 °C to a hexane suspension of 1,1′-dilithioferrocene−TMEDA complex (40 mL), prepared from 0.69 g (3.7 mmol) of ferrocene. The orange precipitate was extracted with dichloromethane, purified by column chromatography (silica gel, dichloromethane−diethyl ether = 7:3), and recrystallized from dichloromethane−hexane (1:1 v/v). The product, **1**, was obtained as an orange solid in 35% yield (0.52 g). Crystals of **1** suitable for single-crystal X-ray analysis were isolated from slow evaporation of an acetonitrile solution at ambient temperature. ^{1}H NMR (250 MHz, $CDCl_3$, 25 °C, TMS) δ: 8.31 (d, 4H, J_{HH} = 4.1 Hz), 6.89 (d, 4H, J_{HH} = 4.1 Hz), 4.55 (m, 4H), 4.50 (m, 4H). IR (KBr, cm^{-1}): 1576(s), 1538(m), 1479(s), 1411(m), 799(s), 704(s), 499(m). Anal. Calcd for $C_{20}H_{16}FeN_2S_2$: C, 59.40; H, 3.99; N, 6.92. Found: C, 59.83; H, 4.04; N 6.81.

1,1′-(2-Dipyridinethio)ferrocene (2). The procedure was similar to that described for the preparation of **1**, except that 1.6 g (7.4 mmol) of 2,2′-dipyridyl disulfide was used instead of 4,4′-dipyridyl disulfide. The product, **2**, was obtained in 60% yield (0.90 g). The method is almost the same as that reported by Laguna et al.[5] ^{1}H NMR (250 MHz, $CDCl_3$, 25 °C, TMS) δ: 8.36 (d, 2H, J_{HH} = 4.9 Hz), 7.42 (t, 2H, J_{HH} = 8.2 Hz), 6.94 (m, 2H), 6.82 (d, 2H, J_{HH} = 8.1 Hz), 4.56 (m, 4H), 4.52 (m, 4H). IR (KBr, cm^{-1}): 1574(s), 1555(s), 1452(s), 1415(s), 1125(s), 762(s), 500(s). Anal. Calcd for $C_{20}H_{16}FeN_2S_2$: C, 59.40; H, 3.99; N, 6.92. Found C, 59.31; H, 3.99; N 6.91.

[Ag{1,1′-(4-dipyridinethio)ferrocene}(PF_6)]$_n$ (3). A methanol solution (2 mL) of $AgPF_6$ (25 mg, 1.0×10^{-1} mmol) was mixed with dichloromethane solution (3 mL) of **1** (40 mg, 1.0×10^{-1} mmol) and stirred for 30 min. The orange precipitate was collected by filtration and washed successively with methanol and dichloromethane. The product was recrystallized from acetonitrile−diethyl ether (1:1 v/v). The product, **3**, was obtained as an orange solid in 49% yield (32 mg). Crystals of **3** suitable for single-crystal X-ray analysis were isolated from slow evaporation of an acetonitrile solution at ambient temperature. IR (KBr, cm^{-1}): 2250(m), 1594(s), 1560(s), 1457(s), 1428(s), 1168(s), 1059(s), 830(s), 762(s), 558(s). Anal. Calcd for $C_{20}H_{16}AgF_6FeN_2PS_2$: C, 38.99; H, 3.00; N, 7.58. Found C, 39.19; H, 3.06; N, 7.48.

[Cu{1,1′-(4-dipyridinethio)ferrocene}$_2$$(PF_6)$]$_n$ (4). $[Cu(CH_3CN)_4]PF_6$ (20 mg, 5.0×10^{-2} mmol) was treated with **1** (40 mg, 1.0×10^{-1}mmol) in dichloromethane (40 mL). After stirring for 30 min, the yellow precipitate was filtered and washed with dichloromethane. The product, **4**, was obtained as yellow solid in 48% yield (29 mg). IR (KBr, cm^{-1}): 1599(s), 1429(s), 1113(s), 1066(s), 841(s), 818(s), 731(s), 557(s), 498(s). Anal. Calcd for $C_{40}H_{32}CuF_6Fe_2N_4PS_2$: C, 47.22; H, 3.17; N, 5.50. Found C, 47.26; H, 3.25; N, 5.46. An attempted crystallization of the product from acetonitrile and diethyl ether (1:1 v/v) resulted in the recovery of the starting materials.

[Mn(hfac)$_2${1,1′-(4-dipyridinethio)ferrocene}]$_n$ (5). A diethyl ether solution (4 mL) of **1** (50 mg, 1.0×10^{-1} mmol) was mixed with dichloromethane solution (4 mL) of **1** (40 mg, 1.0×10^{-1} mmol) for 30 min. The yellow precipitate was filtrated and washed successively with dichloromethane and diethyl ether, and then the precipitate was recrystallized from methanol−diethyl ether (1:1 v/v). The product, **5**, was obtained as a pale orange solid in 67% yield (60 mg). Crystals of **5** suitable for single-crystal X-ray analysis were isolated from slow evaporation of an methanol solution at ambient temperature. IR (KBr, cm^{-1}): 1651(s), 1593(s), 1554(s), 1506(s), 1487(s), 1421(s), 1263(s), 1201(s), 1136(s), 816(s), 793(s), 717(s), 665(s), 582(s), 496(s). Anal. Calcd for $C_{30}H_{18}F_{12}FeMnN_2O_4S_2$: C, 41.25; H, 2.08; N, 3.21. Found C, 41.42; H, 2.18; N, 3.08.

[Cu(hfac)$_2${1,1′-(4-dipyridinethio)ferrocene}]$_n$ (6). A methanol solution (2 mL) of $Cu(hfac)_2$ (50 mg, 1.0×10^{-1} mmol) was slowly layered onto a dichloromethane solution (4 mL) of **1** (40 mg 1.0×10^{-1} mmol) in test tubes at room temperature. Complex **6** was obtained as dark green crystals in 3 days (52 mg, 58%). IR (KBr, cm^{-1}): 1667(s), 1663(sh), 1601(s), 1554(s), 1425(s), 1266(s), 1200(s), 1132(s), 822(s), 790(s), 725(s), 670(s), 499(s). Anal. Calcd for $C_{30}H_{18}CuF_{12}FeN_2O_4S_2$: C, 40.85; H, 2.06; N, 3.18. Found C, 40.83; H, 2.16; N, 3.22.

[Zn(hfac)$_2${1,1′-(4-dipyridinethio)ferrocene}]$_n$ (7). Complex **7** was obtained by a similar procedure to that of **5**, except that $Zn(hfac)_2$ (50 mg, 1.0×10^{-1} mmol) was used instead of $Cu(hfac)_2$. Product **7** was obtained as yellow crystalline solid in 65% yield (59 mg). IR (KBr, cm^{-1}): 1652(s), 1596(s), 1555(s), 1422(s), 1265(s), 1203(s), 1135(s), 820(s), 793(s), 720(s), 670(s), 498(s). Anal. Calcd for $C_{30}H_{18}F_{12}FeN_2O_4S_2Zn$: C, 40.77; H, 2.05; N, 3.17. Found C, 40.89; H, 2.28; N, 3.01.

[Cu{1,1′-(2-dipyridinethio)ferrocene}(PF_6)]$_n$ (8). A dichloromethane solution (5 mL) of $[Cu(CH_3CN)_4]PF_6$ (20 mg, 5.0×10^{-5} mol) was slowly diffused onto a dichloromethane solution (5 mL) of **2** (20 mg, 5.0×10^{-5} mol) in an H-type cell at room temperature. The complex **8** was obtained as yellow crystals in a week in 91% yield (28 mg). IR (KBr, cm^{-1}): 1594(s), 1560(s), 1457(s), 1428(s), 1168(s), 1059(s), 830(s), 762(s), 558(s). Anal. Calcd for $C_{20}H_{16}CuF_6FeN_2PS_2$: C, 39.07; H, 2.95; N, 4.56. Found C, 39.35; H, 2.68; N, 4.55.

X-ray Diffraction Studies. All the X-ray data were collected using Mo Kα radiation on a Rigaku AFC-5S four-circle diffractometer. Crystal data, data collection parameters, and analysis statistics for **1**, **3** and **8**, and **5**−**7** are listed in Tables 1 and 2, respectively. All calculations were performed using the teXsan crystallographic software package.[12] These structures were solved by the direct methods (SIR 92[13] and SHELEX 97[14]) and expanded using Fourier techniques. The non-hydrogen atoms were refined anisotropically. Absorption correction was applied (ψ-scan). Though

(12) *teXsan: Crystal Structure Analysis Package*; Molecular Structure Corporation: The Woodlands, TX, 1985 and 1999.
(13) Altomore, A.; Burla, M. C.; Camalli, M.; Cascarano, M.; Giacovazzo, C.; Guagliardi, A.; Polidori, G. *J. Appl. Crystallogr.* **1994**, *27*, 435.
(14) Sheldrick, G. M. *Program for the Solution of Crystal Structures*; University of Göttingen: Germany, 1997.

Table 1. Crystallographic Data for **1**, **3**, and **8**

	1	**3**	**8**
formula	$C_{20}H_{16}FeN_2S_2$	$C_{24}H_{22}AgF_6FeN_4PS_2$	$C_{20}H_{16}CuF_6FeN_2PS_2$
fw	404.34	739.26	614.85
T/°C	23	23	23
cryst syst	triclinic	triclinic	orthorhombic
space group	$P\bar{1}$	$P\bar{1}$	*Pbcn*
a/Å	9.909(2)	14.006(3)	10.401(3)
b/Å	11.529(2)	14.234(3)	26.428(3)
c/Å	8.096(2)	7.265(3)	8.065(4)
α/°	98.79(2)	103.07(3)	
β/°	98.29(2)	93.77(2)	
γ/°	77.99(1)	94.48(2)	
V/Å^3	890.8(3)	1401.2(7)	2216(1)
Z	2	2	4
ρ_{calcd}/g cm^{-3}	1.537	1.752	1.842
μ/cm^{-1}	10.85	14.82	19.36
R_1[a]	0.034	0.044	0.078
R_w[a]	0.106	0.134	0.235

[a] $R_1 = \sum||F_o| - |F_c||/\sum|F_o|$; $R_w = [\sum w(F_o^2 - F_c^2)^2/\sum w(F_o^2)^2]^{1/2}$.

Table 2. Crystallographic Data for **5**, **6**, and **7**

	5	**6**	**7**
formula	$C_{30}H_{18}N_2O_4F_{12}S_2FeMn$	$C_{30}H_{18}N_2O_4F_{12}S_2CuFe$	$C_{30}H_{18}N_2O_4F_{12}S_2FeZn$
fw	873.37	881.98	883.81
T/°C	23	23	23
cryst syst	triclinic	triclinic	triclinic
space group	$P\bar{1}$	$P\bar{1}$	$P\bar{1}$
a/Å	10.328(2)	10.267(3)	10.295(3)
b/Å	10.763(2)	10.752(4)	10.763(8)
c/Å	8.574(2)	8.378(3)	8.386(6)
α/°	112.88(1)	112.70(3)	112.57(4)
β/°	99.29(2)	100.92(2)	99.01(4)
γ/°	94.19(2)	92.56(3)	93.35(4)
V/Å^3	856.9(3)	830.7(5)	840.3(10)
Z	1	1	1
ρ_{calcd}/g cm^{-3}	1.692	1.763	1.746
μ/cm^{-1}	10.17	13.09	13.75
R_1[a]	0.072	0.059	0.066
R_w[a]	0.243	0.203	0.207

[a] $R_1 = \sum||F_o| - |F_c||/\sum|F_o|$; $R_w = [\sum w(F_o^2 - F_c^2)^2/\sum w(F_o^2)^2]^{1/2}$.

some of the hydrogens were found by means of the Fourier synthesis, all hydrogen atoms were inserted at the calculated positions using a rigid model.

Crystallographic data (excluding structure factors) for the structure reported in this paper have been deposited with the Cambridge Crystallographic Data Centre as supplementary publication nos. CCDC 172378-172383. Copies of the data can be obtained free of charge on application to CCDC, 12 Union Road, Cambridge CB2 1EZ, U.K. (fax (+44)1223-336-033; e-mail deposit@ccdc.cam.ac.uk).

Results and Discussion

Redox-Active Bridging Ligands, 1,1′-(4-Dipyridinethio)ferrocene (1) and 1,1′-(2-Dipyridinethio)ferrocene (2). The bidentate ligands **1** and **2** were synthesized to produce redox-active coordination polymers. Satisfactory analytical data (^{1}H NMR, IR, elemental analysis) were obtained (vide ante). An ORTEP view of the ligand of **1** is shown in Figure 1 with the numbering scheme. Selected bond lengths and angles are listed in Table 3. There are two crystallographically independent molecules in the unit cell. Their geometries differ only very slightly, and both molecules have a center of symmetry at the iron atom site. The pyridyl nitrogen atoms

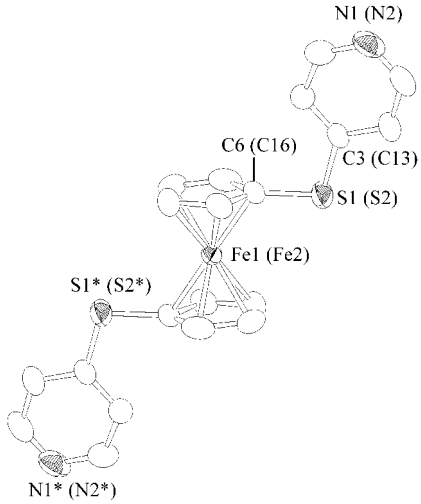

Figure 1. ORTEP drawing of **1** with the atom numbering scheme, showing the molecular structure. Displacement ellipsoids are shown at the 50% probability level. Hydrogen atoms are omitted for clarity. Only one of the two crystallographically independent molecules is shown, with the numbering of the other molecule in parentheses.

Table 3. Selected Bond Lengths (Å) and Bond Angles (deg) with Estimated Standard Deviations in Parentheses

		1	
(molecule A)		(molecule B)	
C(3)−S(1)	1.760(2)	C(13)−S(2)	1.755(2)
C(6)−S(1)	1.757(2)	C(16)−S(2)	1.752(2)
C(3)−S(1)−C(6)	102.73(9)	C(13)−S(2)−C(16)	103.16(9)
		3	
Ag−N(1)	2.181(3)	Ag−N(2)	2.186(3)
C(3)−S(1)	1.771(4)	C(6)−S(1)	1.752(4)
C(13)^{I} [a]−S(2)	1.770(4)	C(16)−S(2)	1.745(4)
N(1)−Ag−N(2)	163.9(1)	C(3)−S(1)−C(6)	100.9(2)
C(13)^{I}−S(2)−C(16)	101.6(2)		
		5	
Mn−N(1)	2.266(4)	Mn−O(1)	2.174(3)
Mn−O(2)	2.141(3)	C(3)−S(1)	1.757(4)
C(6)−S(1)	1.760(6)		
N(1)−Mn−N(1)^{I} [b]	180	N(1)−Mn−O(1)	92.1(1)
N(1)−Mn−O(2)	90.2(1)	C(3)−S−C(6)	102.7(2)
		6	
Cu−N(1)	2.016(3)	Cu−O(1)	2.297(3)
Cu−O(2)	2.004(2)	C(3)−S(1)	1.763(4)
C(6)−S(1)	1.756(5)		
N(1)−Cu−N(1)^{I} [c]	180	N(1)−Cu−O(1)	90.9(1)
N(1)−Cu−O(2)	90.3(1)	C(3)−S−C(6)	102.5(2)
		7	
Zn−N(1)	2.145(4)	Zn−O(1)	2.117(3)
Zn−O(2)	2.082(3)	C(3)−S(1)	1.760(5)
C(6)−S	1.754(6)		
N(1)−Zn−N(1)^{I} [d]	180	N(1)−Zn−O(1)	88.5(1)
N(1)−Zn−O(2)	89.8(1)	C(3)−S−C(6)	102.6(2)
		8	
Cu−N(1)	1.904(8)	C(1)−S(1)	1.769(9)
C(6)−S(1)	1.77(1)		
N(1)−Cu−N(1)^{I} [e]	180	C(1)−S−C(6)	103.0(4)

[a] Symmetry code (I): $x, y - 1, z + 1$. [b] Symmetry code (I): $-x + 1, -y, -z + 1$. [c] Symmetry code (I): $-x + 2, -y, -z + 2$. [d] Symmetry code (I): $-x + 1, -y, -z + 1$. [e] Symmetry code (I): $-x, -y, -z$.

are directed toward opposite directions, manifesting its versatility as a bidentate ligand.

The cyclic voltammograms of **1** and **2** in dichloromethane show half-wave potentials ($E_{1/2}$) at +0.43 and +0.46 V (vs $FeCp_2/FeCp_2^+$), respectively. The ΔE_p values of **1** and **2** are 53 and 57 mV, respectively, which are one-electron redox

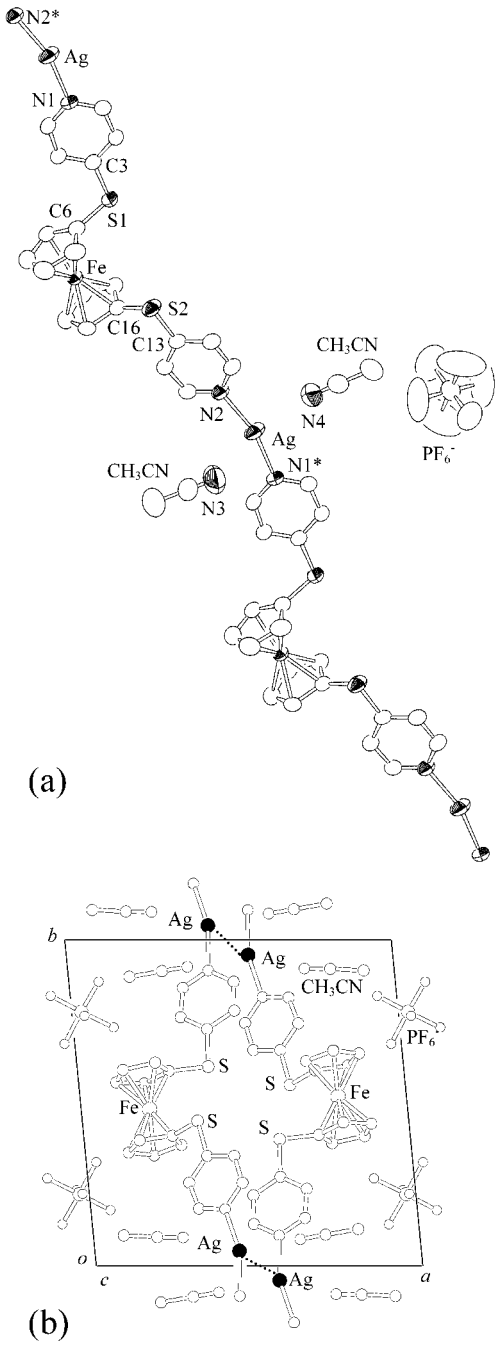

Figure 2. (a) ORTEP drawing of the linear chain structure in **3** with the atom numbering scheme. Displacement ellipsoids are shown at the 50% probability level. Hydrogen atoms are omitted for clarity. (b) Packing diagram of **3** viewed along the *c*-axis. Hydrogen atoms are omitted for clarity.

processes. These positive shifts relative to ferrocene are due to the electron-withdrawing effect of the pyridylthio moiety. In acetonitrile solutions, the cyclic voltammogram showed irreversible oxidation waves, probably because of the coordination of acetonitrile to the iron atom upon oxidation.[15]

One-Dimensional Straight Chain Complex, [Ag{1,1′-(4-dipyridinethio)ferrocene}(PF_6)]$_n$ (3). An ORTEP view of the chain structure of **3** is shown in Figure 2a, with the numbering scheme. Selected bond lengths and angles are listed in Table 3. The chain consists of the alternate linkage of Ag ions and the bridging ligand. The Ag^I coordination in **3** is linear, with a N(1)−Ag−N(2) angle of 163.9(1)°, and Ag−N(1) and Ag−N(2) bond lengths of 2.181(3) and 2.186(3) Å, respectively, which are typical values for Ag−N coordination distances.[8] The complex involves two solvent molecules of acetonitrile around the Ag ion, although the distances from the Ag ion to the nitrogen atoms of acetonitrile, 2.652(6) and 3.022(7) Å for Ag−N(3) and Ag−N(4), respectively, are long for significant Ag^I−N interactions.[16] The stretching frequency ν(C═N) of the guest molecule was observed at 2250 cm^{-1} in the infrared spectrum. Thermogravimetric analysis of **3** exhibits loss of the two acetonitrile molecules between ∼80−120 °C in one step (11.65% weight loss observed; 11.11% calculated).

The packing structure of **3** is shown in Figure 2b. The chain structure extends along the *b*-axis, and the distance between the Ag ions along the chain is 17.36 Å. It is noted that a relatively short Ag···Ag distance (=3.2670(8) Å) is found between two adjacent chains, and thus, the structure may be regarded as a double-chain one. The ferrocene moieties of **3** are located on the same side of individual chains, and we speculate that the weak Ag···Ag interactions[17] in adjacent chains may play the role of orienting the ferrocene moieties. Solids of **3** showed no significant emission in the range 400−800 nm, although some compounds with short Ag···Ag distances exhibit fluorescence due to d^{10}−d^{10} *aurophilic* interactions.[18] We found that ligand **1** also forms a complex represented as $\mathbf{1}_2$·$CuPF_6$ (**4**), which we failed to crystallize.

One-Dimensional Straight Chain Complex, [M(hfac)$_2$-{1,1′-(4-dipyridinethio)ferrocene}]$_n$ (M = Mn (5), Cu (6), Zn (7)). Complexes **5**−**7** assume one-dimensional straight chain structures, which consist of the alternate linkage of M(hfac)$_2$ and the ligand. An ORTEP view of the chain structure of **5** is shown in Figure 3a with the numbering scheme. Compounds **6** and **7** are isomorphous to **5**. Selected bond lengths and angles are listed in Table 3. In these complexes, the metal ion of M(hfac)$_2$ is hexacoordinated by the four oxygen atoms of the hfac ligands and the two N-donor atoms of **1** occupying the trans positions. The coordination geometries of these complexes are listed in Table 3. The Cu−O(1) distance of 2.297(3) Å in **6** is slightly longer than the other M−O distances because of the Jahn−Teller effect. The IR spectrum of **6** shows two carbonyl stretching bands at 1667 and 1663 cm^{-1}, in accord with the

(15) Ogino, H.; Tobita, H.; Habazaki, H.; Shimoi, M. *J. Chem. Soc., Chem. Commun*. **1989**, 828−829.

(16) (a) Janiak, C.; Uehlin, L.; Wu, H.-P.; Klüfers, P.; Piotrowski, H.; Scharmann, T. G. *J. Chem. Soc., Dalton Trans*. **1999**, 3121−3131. (b) Bachman, R. E.; Andretta, D. F. *Inorg. Chem*. **1998**, *37*, 5657−5663.

(17) (a) Yaghi, O. M.; Li, H. *J. Am. Chem. Soc*. **1996**, *118*, 295−296. (b) Tong, M.-L.; Chen, X.-M.; Ye, B.-H. *Inorg. Chem*. **1998**, *37*, 5278−5281. (c) Yang, S.-P.; Zhu, H.-L.; Yin, X.-H.; Chen, X.-M.; Ji, L.-N. *Polyhedron* **2000**, *19*, 2237−2242. (d) Robinson, F.; Zaworotko, M. J. *J. Chem. Soc., Chem. Commun*. **1995**, 2413−2414. (e) Jung, O.-S.; Park, S. H.; Park, C. H.; Park, J. K. *Chem. Lett*. **1999**, 923−924. (f) Carlucci, L.; Ciani, G.; Gudenberg, D. W. v.; Proserpio, D. M. *Inorg. Chem*. **1997**, *36*, 3812−3813.

(18) (a) Catalano, V. J.; Kar, H. M.; Bennett, B. L. *Inorg. Chem*. **2000**, *39*, 121−127. (b) Harvey, B. L.; Gray, H. B. *J. Am. Chem. Soc*. **1988**, *110*, 2145−2147.

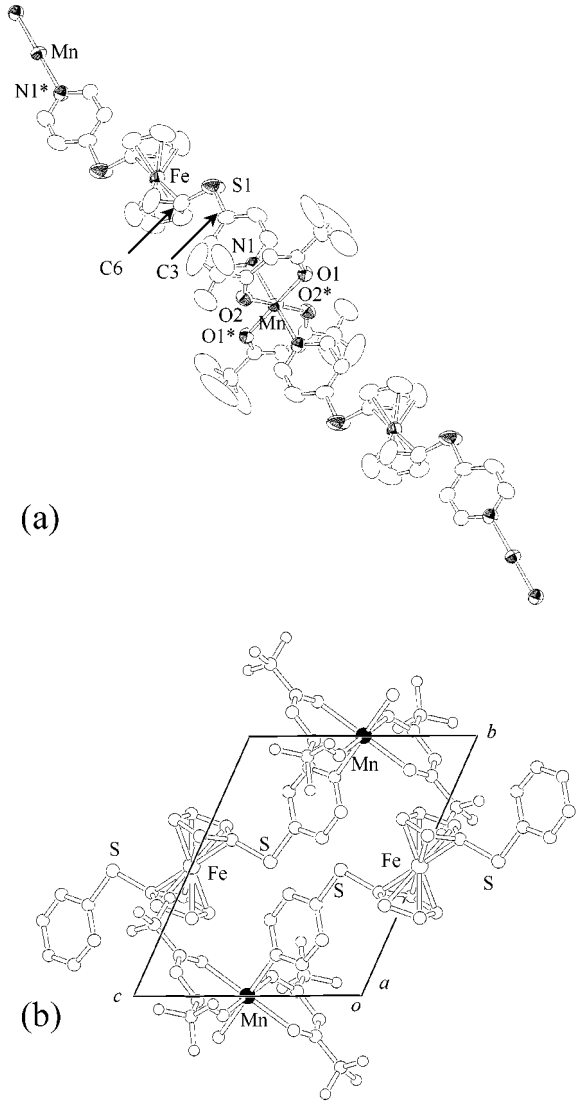

Figure 3. (a) ORTEP drawing of the linear chain structure in **5** with the atom numbering scheme. Displacement ellipsoids are shown at the 50% probability level. (b) Packing diagram of **5** viewed along the *a*-axis. Hydrogen atoms are omitted for clarity.

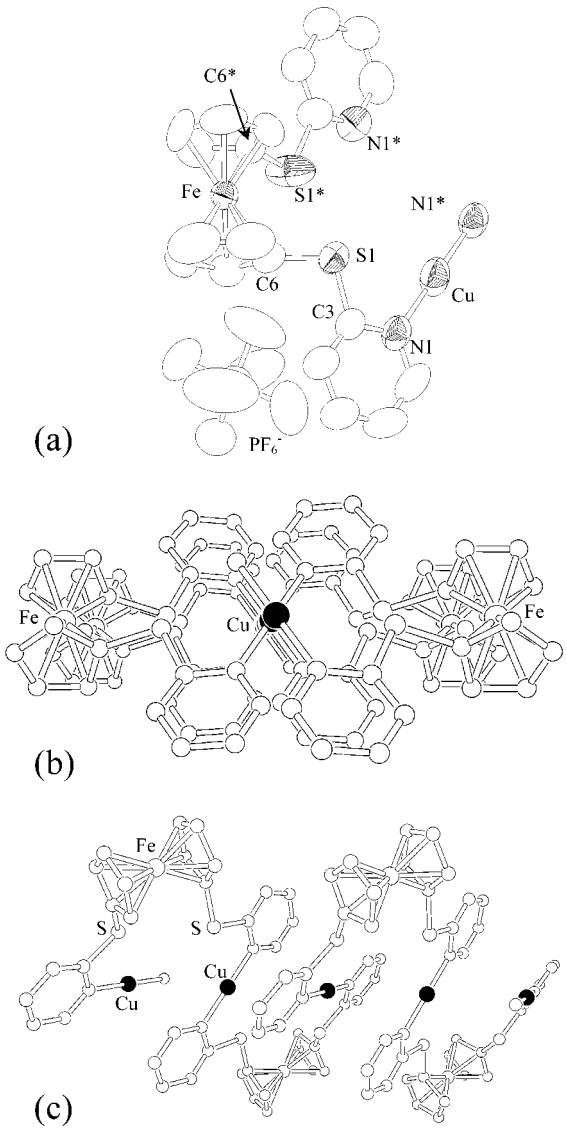

Figure 4. (a) ORTEP drawing of **8** with the atom numbering scheme, showing the copper coordination environment. Displacement ellipsoids are shown at the 50% probability level. Hydrogen atoms are omitted for clarity. (b) Structure of one-dimensional twisted helix-like chain in **8** viewed along the copper array. Cu atoms are shaded. (c) Side view of the twisted helix-like chain in **8**.

X-ray structure showing two types of Cu−O distances.[9a] On the other hand, compounds **5** and **7** show the carbonyl stretching bands at 1651 and 1652 cm^{-1}, respectively, as single peaks.

The packing structure of **5** is shown in Figure 3b. In complexes **5**−**7**, the straight chains run along the [111] direction, and there are no interchain interactions of any note. The intrachain M···M separations are 18.86, 18.39, and 18.66 Å for **5** (M = Mn), **6** (M = Cu), and **7** (M = Zn), respectively, which are longer than the nearest interchain separations for the corresponding complexes, 8.57, 8.38, and 8.39 Å, respectively.

The magnetic susceptibilities of **5** and **6** were measured by using a SQUID susceptometer. These complexes are simple paramagnets with negligible intermolecular interactions. The susceptibilities obey the Curie−Weiss law, with the Weiss constants of −0.4 K and −0.06 K, for **5** and **6**, respectively, and no cooperative phenomena are observed within the temperature range 300−2 K. The paramagnetic behaviors are consistent with the crystal structures in which the metal−metal distances are too long for significant magnetic interactions.

One-Dimensional Twisted Helix-Like Chain Complex, [Cu{1,1′-(2-dipyridinethio)ferrocene}$(PF_6)]_n$ (8). An ORTEP view of **8** is shown in Figure 4a with the numbering scheme. Selected bond lengths and angles are listed in Table 3. The coordination environment of Cu^I in **8** is linear, with an N(1)−Cu−N(1*) angle of 180°, and a Cu−N(1) bond length of 1.904(8) Å, which are typical values in copper complexes with a linear coordination geometry. The Cu···S separation distance is 2.96 Å, which is too long for significant Cu−S interactions.

It is interesting to note that ligand **2** also afforded a one-dimensional coordination polymer. Figure 4b,c shows the helix-like chain structure of **8**. In contrast to the straight chain structures in **3**−**7**, the helix-like chain in **8** is highly twisted.

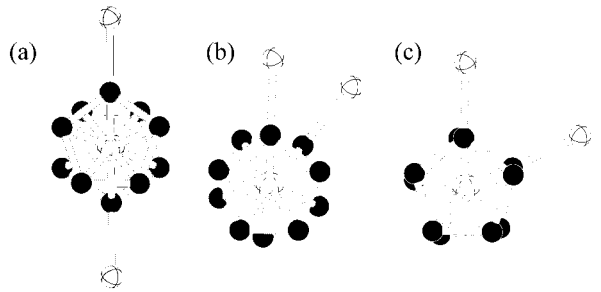

Figure 5. Conformations of the ferrocenyl rings in **1**, **3**, and **5**−**8**. (a) **1**, **5**−**7** (antiperiplanar), (b) **3** (synclinal, staggered), (c) **8** (synclinal, eclipsed).

Table 4. Structural Parameters of the Ferrocenyl Rings

cmpd	Fe−Cp distance/Å	torsion angle/deg [a]	conformation
1	1.646(1), 1.642(2)	180	antiperiplanar
3	1.643(3), 1.645(2)	40	synclinal (staggered)
5	1.632(5)	180	antiperiplanar
6	1.638(4)	180	antiperiplanar
7	1.638(5)	180	antiperiplanar
8	1.642(3)	65	synclinal (eclipsed)

[a] $C_A-X_A-X_B-C_B$ torsion angle/deg, where C_A is a carbon atom in Cp(A) ring that is bonded to the S atom (likewise for C_B) and X_A and X_B are the centroids of the two Cp rings A and B, respectively.

In this complex, the Cu atom lies on an inversion center, and the Fe and P atoms lie on independent 2-fold axes. The twist pitch of the helix is 8.07 Å (cyclical Cu···Cu separation), and the cyclical Fe···Fe separation is 12.09 Å. The interchain Cu···Cu separation (4.03 Å) is shorter than the intrachain separation (14.87 Å).

Very recently, the group of Laguna reported interesting coordination complexes of this ligand with Au^I and Ag^I ions. Their complex of $Ag_2L_3(OTf)_2$ shows a symmetrical structure, in which three ligands are bridging two Ag^I ions. On the other hand, our Cu^I coordination polymer shows a helix-like chain structure, with a highly twisted configuration. Such an interesting structural variation may be derived from the conformational flexibility of the ferrocene-based ligand.

Conformation of the Ferrocenyl Rings in 1−8. In all of the previously described complexes, the distances from the iron atom to the Cp planes are around 1.64 Å, which is a typical value for a neutral ferrocene moiety.[19] The conformations of the ferrocene moieties in **1**−**8** are shown in Figure 5. As listed in Table 4, the conformations of disubstituted ferrocenes are classified into six categories in terms of the torsion angle of $C_A-X_A-X_B-C_B$.[20] The conformations of the two Cp rings are antiperiplanar for **1**, **5**, **6**, and **7**, synclinal (staggered) for **3**, and synclinal (eclipsed) for **8**. The conformational freedom of the ferrocenyl moiety in ligands **1** and **2** may play an important role in the formation of these coordination polymers.

Solid-State Redox Properties of 1−8. Solid-state cyclic voltammograms of **1**, **3**, and **5** are shown Figure 6, and the redox potentials are listed in Table 5. The voltammogram of **2** is similar to that of **1**, and those for **6** and **7** are similar

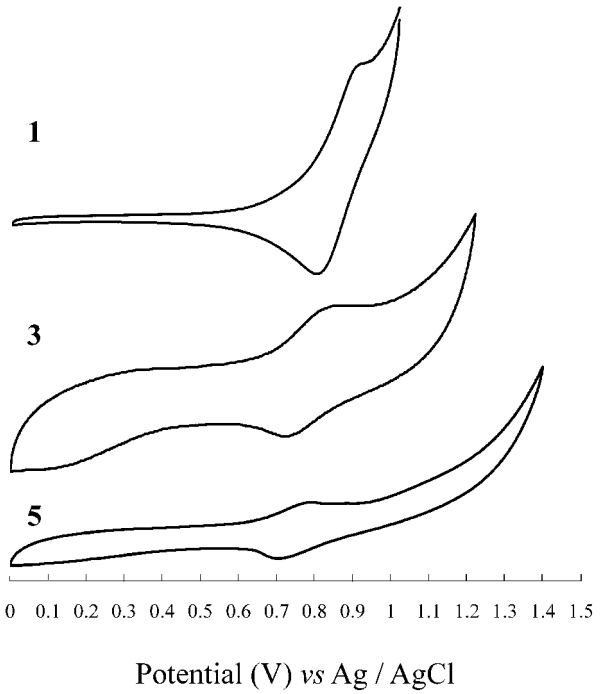

Figure 6. Solid-state cyclic voltammograms (vs. Ag/AgCl) of **1**, **3**, **5**, and **7**.

Table 5. Solid State Redox Potentials from Cyclic Voltammetry (in V vs $FeCp_2/FeCp_2^+$)

cmpd	$E_{1/2}$	E_{pa}	E_{pc}
1	0.50	0.56	0.45
2	0.51	0.61	0.40
3	0.42	0.46	0.37
5	0.43	0.47	0.40
6	0.39	0.40	0.37
7	0.43	0.46	0.40

to that of **5**. The observed redox peaks correspond to the redox processes of the ferrocene moieties. The complexes **1** and **2** showed half-wave potentials ($E_{1/2}$) at 0.50 and 0.51 (vs solid-state $FeCp_2/FeCp_2^+$), which are slightly shifted by ca. +0.06 V from those in solutions. As listed in Table 5, the half-wave potentials ($E_{1/2}$) for **3** and **5**−**7** were obtained at around 0.4 V (vs solid-state $FeCp_2/FeCp_2$+), which are shifted negatively with respect to that of **1** in the solid state. These negative shifts may be attributed to the relative stabilization of the oxidized species in the coordination polymers, which has anionic moieties such as $hfac^-$ and PF_6^- located nearby the ferrocene moieties. In addition, various ΔE_p values of each sample are 0.03−0.21. On the other hand, we could not observe clear redox peaks for complex **8**, which is probably because of the air sensitivity of the surfaces of the complex, for it contains Cu^I. Actually, we found that complex **8** decomposes gradually under air, while the other complexes are highly stable.

Conclusion

We have shown that the reaction of ferrocene-based bridging ligands with metal ions leads to the formation of several redox-active coordination polymers. The conformational flexibility of the ligand may have led to the various assembled structures of the present complexes. The approach

(19) Seiler, P.; Dunitz, J. D. *Acta Crystallogr., Sect. B* **1979**, *B35*, 2020−2032.
(20) Mai, J.-F.; Yamamoto, Y. *J. Organomet. Chem.* **1998**, *560*, 223−232.

of incorporating functional groups into the bridging ligands may further lead to the construction of interesting assembled complexes.

Acknowledgment. We thank Prof. H. Mori (ISSP, the University of Tokyo) and Mr. H. Suzuki (Toho University) for their help in measuring magnetic susceptibilities. We also thank Mr. M. Itou for supporting our research activities and Ms. Y. Sato (School of Pharmaceutical Sciences, Toho University) for elemental analyses. We are grateful to Prof. M. Hasegawa (Toho University) for TG analysis and fluorescence measurements. This work was performed using facilities of the Institute for Solid State Physics, the University of Tokyo.

Supporting Information Available: Tables of detailed crystallographic data, atomic positional parameters, anisotropic displacement parameters, and bond length and angles in CIF format. This material is available free of charge via the Internet at http://pubs.acs.org.

IC011176K